DOR: 20.1001.1.2322388.2020.8.3.4.7

Research Paper

New Iteration based Algorithm for Shape Optimization of Internal and External Boundaries of the Initial Blank in the Deep Drawing Process

Hamidreza Gharehchahi[1], Mohammad Javad Kazemzadeh-Parsi[*2], Ahmad Afsari[2], Mehrdad Mohammadi[3]

1. Ph.D. Student, Department of Mechanical Engineering, Shiraz Branch, Islamic Azad University, Shiraz, Iran.
2. Associate Professor, Department of Mechanical Engineering, Shiraz Branch, Islamic Azad University, Shiraz, Iran.
3. Assistant Professor, Department of Mechanical Engineering, Shiraz Branch, Islamic Azad University, Shiraz, Iran

ARTICLE INFO

Article history:

Received 24 November 2019
Accepted 5 January 2020
Available online 22 July 2020

Keywords:

Deep drawing
Shape optimization
Blank optimization
Finite element method

ABSTRACT

In the deep drawing process, the optimal design of the initial blank shape has many advantages such as reducing the cost of production and waste and improving the quality of the process and thickness distribution. The deep drawing process is highly nonlinear due to the large deformation, plastic deformation of the material and the contact phenomenon. Therefore, the general solution to such problems is to use iterative methods based on numerical simulation. The present study implements a similar approach and presents a new algorithm to make geometrical corrections to the external boundaries of a blank, as well as its internal boundaries, in several iterations. A computer program was developed to automatically run these iterations to study the features of the proposed algorithm. Next, an example problem was solved, and the results are compared with other studies. The results showed that the proposed algorithm is sufficiently robust against the initial guesses for the blank, which is an advantage of the present algorithm over those from other algorithms. Because in other algorithms presented in the articles, if the appropriate initial guess is not selected, the algorithm will not converge to the answer. The proposed algorithm also has a higher convergence speed in achieving optimal blank.

* **Corresponding Author:**
Email Address: kazemzadeh@iaushiraz.ac.ir

1. Introduction

Deep drawing is a useful sheet metal forming process for shaping flat blanks into cup-like forms. The process begins by cutting the blank with a specific geometry and placing it on the die. The plunging of the punch into the die drives the blank in, forming it into the shape of the die. Often, the part of the blank that remains outside does not develop a favorable shape and should be recut. The second cutting process creates two main issues of increasing wastes and involving complexities that can raise the production cost. Therefore, production costs remain lower if additional cutting can be avoided or at least minimized. An optimum blank geometry can realize this objective. Blank optimization refers to selecting an initial blank geometry that develops the desired shape after deep drawing without or with minimal need for additional cutting. Regarding the time-consuming and costly nature of the trial and error-based blank optimization methods, researchers have attempted to use numerical approaches to designing an optimum blank. The use of blanks with optimum geometries offers many advantages in deep drawings, such as reducing the production cost, improving the process quality, thickness distribution, and formability of the part, minimizing forming defects such as wrinkling and rupture and decreasing the number of trial and error steps in the product development process. The numerical simulation of the sheet metal forming process is integral to the study of the feasibility of production by deep drawing and the initial design of a new part with complex three-dimensional geometry. So far, various optimization algorithms have been proposed to design blanks, the most notable algorithms of which can be classified into four groups:

The first group is based on slip line field theory. The initial work done by the slip line field method was done by Hazek et al. [1] in 1979, Lange et al. [2] in 1983 and Sowerby et al. [3] in 1988. They used the field theory of plate strain lines to design the shape of the blank and the materials were considered completely plastic and isotropic. In 1989, Karima [4] calculated the volume of each page element returning from the shape of the final container to the position of the main blank for each advance follows the punch. In 1990, Vogel and Lee [5] introduced an analysis method for designing a deep drawing process based on the plate stress characteristic theory. In 1992, Chen and Sowerby [6] proposed the development of ideal blank shapes by the plane stress characteristic method, which neglects natural and shear stresses acting on the thickness of the material, as well as changes in the thickness of the in-plane stresses. In 1996 Chen et al. [7] performed a similar analysis to trace the blank shape. In 1997 Kuwabara et al. [8] also proposed a method based on this theory. Acceptable kinetic velocity field for the flange region is determined by theory and this velocity field is used to calculate the return of material flow from the flange shape. Optionally executed in the form of blank. They make the radius of the punch and the corner of the die zero and the material is isotropic and completely rigid plastic. Also, the thickness of the blank was assumed to be constant during the process. In 2004, Parsa et al. [9] Use conventional methods to construct slip lines around the die housing. Using the constructed slip lines, a curve is drawn that defines the circumference of the initial blank. To reduce the distance between the start and end point of the curve of the initial blank, they used the new rule to divide the shape of the original blank.

The second group is based on the geometric mapping. In 1986, Kim et al. proposed an approximate geometric method for determining the shape of a blank contour for drawing a rectangular container [10]. Experimental parameters of the velocity field are assumed. The flow lines of the material points in the blank are related, and the flange contour is determined for the shape of the given blank in several advances of the punch, assuming the material isotropic. In 1986, Sowerby et al. [11] analyzed sheet metal stamping modeling by measuring the node points of the lattice marked on the deformed plate to determine the strain distribution. In 1995, Blount and Fischer [12] made blank computer-aided predictions for sheet metal components with double curved surfaces. In 1998, Zaky et al. determined the optimal shape of the blank for deep drawing of the corner cylindrical container [13]. They used the concept of normal anisotropy ratio values that are not constant over the entire amplitude of the crystallographic rotation.

The third group is based on the inverse approach. In 1992, Chang et al. proposed a theoretical basis for the theory of ideal shaping to achieve the shape of the initial blank [14]. However, real forming conditions such as blank holder force, friction force, tool geometry, etc. were not considered. Therefore, the shape of the blank was not accurate enough. In the same year, Iseki and Sowerby [15] determined the desired blank shape when deep drawing symmetrically Non-matched cups using the finite element method. They used an inverse finite element technique to perform the analysis to calculate the blank shapes. In 1996, Barlat et al. [16] performed the optimum blank design of blank contours using the inverse approach and a mathematical programming technique. Blank design and strain prediction of automobile stamping parts by an inverse finite element approach were performed by Lee and Huh in

1997 [17]. In 2000, Guo et al. proposed a finite element inverse method for determining the blank contour in industrial components [18]. This approach uses fragment knowledge by discretizing the three-dimensional plane into the triangular shell elements and calculating the inverse deformation gradient tensor to estimate large logarithmic strain. In 2001, Ku et al. applied the pattern of following the retrogressive to the design of the initial blank [19]. In 2004, Naceur et al. proposed a blank optimization method based on the link between the inverse approach used to simulate the evolutionary algorithm [20]. In 2007, Cai et al. Introduced a simplified algorithm to create a custom 3D surface expansion for the design of blank metal parts [21]. The three-dimensional plane is first divided into triangular elements, the deformation from the curved plane to the wide plane is then done by simulating the plane strain of the main edges. In the same year, Parsa et al. Introduced a modified kinetic relation for predicting the initial blank and used this rule in conjunction with the ideal forming theory to predict the initial blank shape of parts [22]. In 2008, Azizi et al. developed a linear inverted finite element method for optimal blank sheeting [23]. To reduce the computational time, the piece is properly spread on a flat sheet and treated like two-dimensional problems. In the following year, Azizi also compared the basic capabilities of linear and nonlinear relativity of the linear inverse finite element method [24]. The computational time used in linear correlation was significantly shorter than nonlinear correlation.

The fourth group is numerical simulation based iterative methods. In 1985, the study of Toh et al. [25] can be named as one of the earliest papers published on the application of numerical simulation-based iterative methods for blank optimization in deep drawing. The authors relied on a finite element method in the numerical simulation of the deep drawing process, using a geometric correction algorithm based on the flow of material. The main shortcoming of this method is that material flow patterns are not a reliable reference for developing the geometric correction algorithm due to the nonlinear behavior prevalent in deep drawing. The reason lies in the fact that this method fails to converge when the initial guess is far from the optimum. In 1997, Chung et al. [26] developed a sequential design method drawing on the ideal forming theory, finite element analysis, and experimental investigation. They applied the method to design blanks from a severely anisotropic aluminum sheet to minimize corners. In 1999, Park et al. [27] proposed a blank design method by combining the ideal forming method with a deformation path iteration method based on finite element analysis. First, a test blank was prepared based on the ideal forming theory. Then, the optimum blank was obtained by the iterative deformation path iteration method. Although this method is applicable in cases where the depth of drawing and sheet deformation are limited, it reduces the rate of convergence in case of high depth of drawing and severe deformation. Pegada et al. [28], in 2002, used the iterative design procedure in an algorithm to detect optimum blank contours, considering anisotropy and friction in the deep drawing of an aluminum cup. In the same year, Shim et al. [29] used the method of iterative sensitivity for blank optimization. In this method, sensitivity was calculated by finite element analysis of deformation using both main and offset blanks. In 2003, Son et al. [30] proposed the initial velocity of boundary nodes (INOV) method. In this method, the ratio of the initial velocity boundary nodes to the entire path was used in the optimized blank algorithm. In 2008, Vafaeesefat [31] used iteration and the finite element simulation for blank optimization. His blank correction algorithm was based on the projection of the target contour over the deformed blank (boundary projection method). In the same year, Azaouzi et al. [32] introduced an initial blank estimation method based on the one-step inverse approach. Drawing on iterations and by integrating heuristic optimization algorithms with finite element analysis, the authors managed to optimize the blank geometry. In a 2009 study, Hammami et al. [33] developed an iteration-based method working with an experimental initial blank using the Push–Pull design optimization technique. The group also studied the effect of initial anisotropy in obtaining the initial blank shape [34]. In 2002, Fazli et al. [35] proposed a novel iteration based blank optimization technique. This method is described in the next section.

Meanwhile, methods of the fourth category have been widely used by researchers, due to their higher simulation accuracy and more capacity to solve complex problems. The iterative methods are capable of simulating complex geometries, large deformations, complex material behavior models, complex friction models, complex contact models, dynamic behaviors, and other factors with high accuracy. However, demanding a large volume of calculations is the main drawback of numerical simulation-based iterative methods. Developing efficient optimization algorithms can reduce the number of iterations and computational complexity.

In addition to the above sources, new research has been conducted, which is mentioned in the following three cases. In 2020, Zhanga et al. [39] Designed a

blank geometry for reinforced carbon fiber using finite element analysis and presented an innovative approach to automated network tuning integration. They showed that this newly developed approach could accurately design blank geometry under different process conditions. In 2020, Yaghoubi and Fereshteh-Saniee [40] optimization of the geometrical parameters for elevated temperature hydro-mechanical deep drawing process of 2024 aluminum alloy did using a group data management method and bee algorithm to achieve optimal values for process variables. Experimental, numerical and multi-objective optimization studies on the energy absorption features of single- and bi-layer deep-drawn cups were performed by Ghasemabadi et al. In 2020 [41]. In this study, they performed a multi-objective optimization of specific energy absorption and initial peak force based on the polynomial response level.

One issue that the above algorithms face is the inefficiency of the algorithm when the initial guess is far from the optimum blank shape. In other words, the algorithm fails to converge if not provided with a near-optimum initial guess. As a result, the main objective of the present study is to achieve an algorithm that can solve the optimization problem regardless of the initial guess it begins with. The deep drawing process was numerically simulated, and the proposed algorithm was implemented by the finite element method using the commercial software, ABAQUS. Further, the optimization algorithm was programmed by Python. In the end, a numerical example was solved based on the methods of Hammami et al. [33], Fazli et al. [35], and the proposed algorithm, comparing the results to investigate the efficiency of the proposed method. Further, to show that the proposed algorithm is capable of converging to a favorable solution regardless of the initial guess, two numerical examples were solved, the results comparing with the literature.

The present study aims to propose a new, efficient, iteration-based algorithm and implement it by a finite element numerical method to resolve some of the issues related to such methods. The proposed algorithm is classified as an iterative method and is based on numerical simulation.

2. Iterative Method Based Blank Shape Optimization Algorithms

Shape optimization is classified as a variable-domain problem and requires the geometry of the problem domain to be determined as part of the solution process. In these problems, the unknown boundaries are often parametrized for searching in a space with a limited number of dimensions, which is done by selecting a specific number of key points on the boundary and connecting them. The unknown boundary consolidates when the coordinates of the key points are found. Overall, the boundary parameterization technique is commonly used in problems with a variable domain to reduce the number of unknown variables and simplify the solution. Examples of boundary parameterization can be found in the literature [36-37]. In the present study, the boundary was parameterized by selecting a few key points and connecting them with straight lines.

Solving shape optimization problems by numerical simulation based iterative methods starts with an initial guess. Then, the behavior of the model is evaluated through numerical simulation, and the domain geometry is adjusted accordingly. The process continues until the objective of the problem is realized. The present study also takes a similar path. First, an initial guess was drawn for the blank shape here referred to as the initial contour. Then, a deep drawing process was simulated based on the same initial guess, obtaining the final shape of the part (ultimate contour). The final contour does not match the target contour at this stage. As a result, the mismatch between the final and target contours can be quantified by defining an error parameter. The geometry of the initial contour is corrected, and the deep drawing process is simulated again for the algorithm to continue and reduce the error. The process is repeated until convergence when the error drops below a set level. The general flow chart of the optimization steps, explained here, is illustrated in Fig. 1.

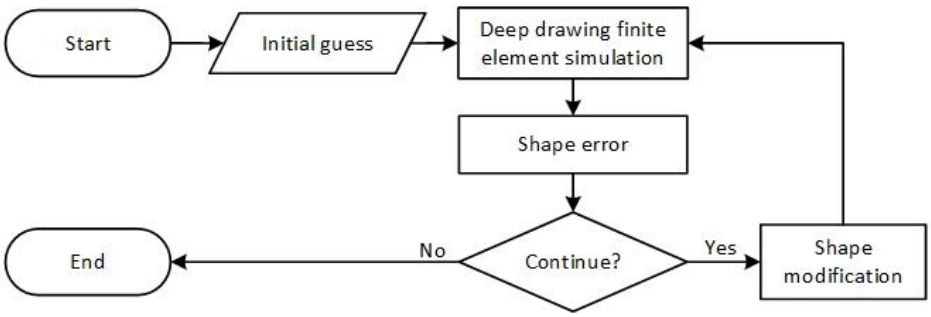

Fig. 1. The flow chart of blank optimization by the iterative method is based on numerical simulation.

Given that the different stopping criteria presented in the literature make the results impossible to compare, the same stopping criterion is used for all algorithms in this study, calculating the Distance of Boundary Node (DBN) to the target contour. Iterations terminate when the DBN is below a set limit for all boundary nodes, indicating that the optimum blank has been achieved. The same also holds for the authors' proposed algorithm.

In the following, the Push–Pull method of Hammami et al. [33] and the extension method of Fazli et al. [35] for blank optimization are discussed along with the new correction algorithm, explaining their processes.

2.1. The Push–Pull Algorithm

The idea for this algorithm was developed by Hammami et al. [33]. See Fig. 2 for the algorithm showing the deformation path of the two boundary nodes. The initial contour is represented by the thin solid line, the final contour by the dashed line, and the target contour by the thick solid line. As evident from the figure, the final contour can be different from the target contour and fall inside or outside of it after the deep drawing. The desired shape after forming can be obtained by adjusting the initial boundary nodes so that all boundary nodes are located within a specified tolerance of the target contour.

Finite element analysis was carried out for the deep drawing process, and the finite element simulation results were obtained in n intervals. Figure 2 shows the deformation path of the boundary nodes I and K as a result of deep drawing at the pth iteration of the blank optimization process. $\vec{X}_{i,p}^{\,j}$ is the position vector of the ith node on the blank boundary at the jth deep drawing interval and the pth iteration of the blank optimization algorithm. The line passing through $\vec{X}_{i,p}^{\,0}$ and $\vec{X}_{i,p}^{\,n}$ crosses the target contour at the intersection point $\vec{X}_{i,p}^{\,inter}$. Then, Geometric Shape Error (GSE) is used to calculate the difference between the final and target contours. The GSE is the root mean square of the difference between the target and final contours and is calculated according to Eq. 1 [33].

$$GSE = \sqrt{\sum_{i=1}^{n} \frac{1}{n} \left| \vec{X}_{i}^{\,inter} - \vec{X}_{i}^{\,n} \right|^2} \quad (1)$$

As long as *GSE* remains higher than the present value, the initial position of the corresponding node $\vec{X}_{i,p}^{\,0}$ must be corrected according to *Eq. 2*.

$$\vec{X}_{i,p+1}^{\,0} = \vec{X}_{i,p}^{\,0} + \xi(\vec{X}_{i,p}^{\,inter} - \vec{X}_{i,p}^{\,n}) \quad (2)$$

The under-relaxation factor ξ shows the stability of the algorithm and is recommended by [9] to be assumed at *0.6*.

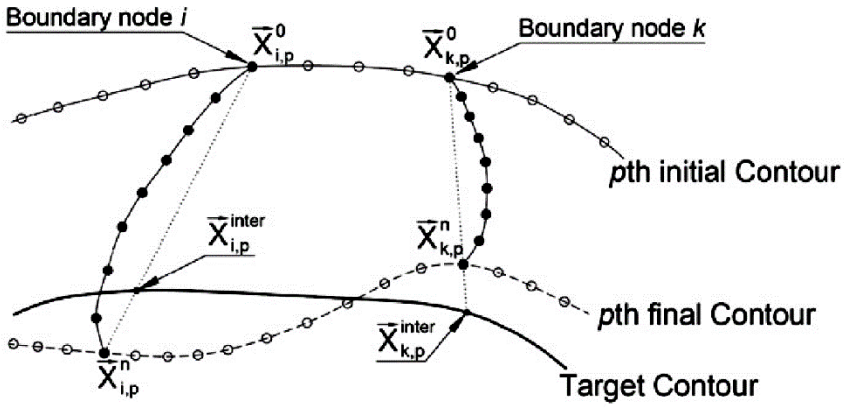

Fig. 2. The deformation path of two boundary nodes in the *Push–Pull* algorithm [33].

2.2. The Extension Algorithm

The idea for this algorithm was developed by Fazli et al. [35]. The function of the algorithm is illustrated in Fig. 3.

The line passing through $\vec{X}_{i,p}^{\,n-1}$ and $\vec{X}_{i,p}^{\,n}$ crosses the target contour at the intersection point $\vec{X}_{i,p}^{\,inter}$. Shape error $\varepsilon_{i,p}$ is defined as the distance between $\vec{X}_{i,p}^{\,inter}$ and $\vec{X}_{i,p}^{\,n}$, is found from Eq. 3.

$$\vec{X}_{i,p}^{\,n} + \varepsilon_{i,p}\hat{r}_{i,p} = \vec{X}_{i,p}^{\,inter} \quad (3)$$

$\hat{r}_{i,p}$ represents the unit vector passing over $\vec{X}_{i,p}^{\,n-1}$, $\vec{X}_{i,p}^{\,n}$ and is obtained from Eq. 4.

$$\hat{r}_{i,p} = \frac{\vec{X}^{n}_{i,p} - \vec{X}^{n-1}_{i,p}}{\left|\vec{X}^{n}_{i,p} - \vec{X}^{n-1}_{i,p}\right|} \quad (4)$$

If the shape error exceeds a specified level at all boundary nodes, the position $\vec{X}^{0}_{i,p}$ is repeatedly corrected until the shape error is reduced below that level. The DBN is the stopping criterion for this algorithm as well, so the algorithms can be compared. The position $\vec{X}^{0}_{i,p}$ is corrected relying on Eq. 5.

$$\vec{X}^{0}_{i,p+1} = \vec{X}^{0}_{i,p} + \varepsilon_{i,p} C_{i,p} \hat{R}_{i,p} \quad (5)$$

$C_{i,p}$ represents the shape error coefficient, and $\hat{R}_{i,p}$ is the unit vector of the line crossing $\vec{X}^{0}_{i,p}$, $\vec{X}^{1}_{i,p}$ and is obtained from Eq. 6.

$$\hat{R}_{i,p} = \frac{\vec{X}^{1}_{i,p} - \vec{X}^{0}_{i,p}}{\left|\vec{X}^{1}_{i,p} - \vec{X}^{0}_{i,p}\right|} \quad (6)$$

It must be noted that, according to Eq. 3 the shape error $\varepsilon_{i,p}$ can be either positive or negative. If the ith node finally takes a position on the target contour (the ith node from Fig. 3), then $\varepsilon_{i,p}$ is negative. Therefore, the initial position of the node moves in the opposite $\hat{R}_{i}$ direction (Eq. 6) and toward the inside of the blank design produced in the previous iteration.

Equation 7 defines the shape error coefficient $C_{i,p}$.

$$C_{i,p} = \beta_{1,p} \frac{\left|\varepsilon_{i,p}\right|}{\sum_{j=1}^{no.\,of\ stages}\left|\vec{X}^{j}_{i,p} - \vec{X}^{j-1}_{i,p}\right|} + \beta_{2,p} \quad (7)$$

The denominator of the above equation is the length of the deformation path of the ith node. $\beta_{1,p}$ and $\beta_{2,p}$ are tuned so $C_{i,p}$ remains between 0.5 and 0.9 [6]. The values are calculated in every iteration and are similar for all nodes. The minima and maxima of Eq. 7 are calculated for all boundary nodes to determine $\beta_{1,p}$ and $\beta_{2,p}$. The minimum of the relation is 0.5 while the maximum is 0.9. The two equations and two unknowns determine $\beta_{1,p}$ and $\beta_{2,p}$.

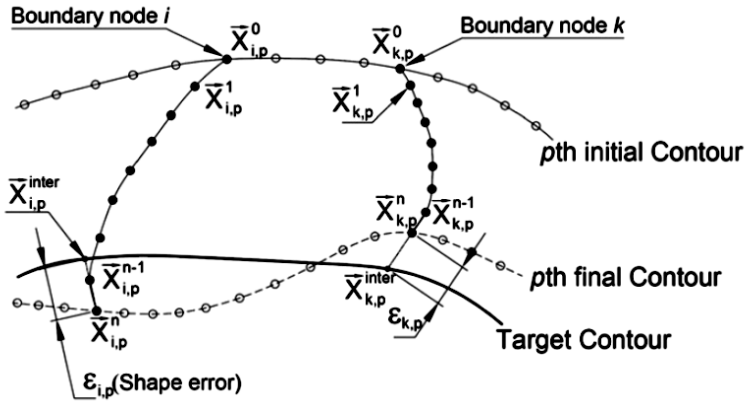

Fig. 3. The deformation path of two boundary nodes in the *Extension* algorithm [35].

In the present study, $C_{i,p}$ was considered the stability factor of the algorithm and was assumed equal to ξ for the algorithms to be compared. In other words, it ξ was assumed at 0.6 in the example, $C_{i,p}$ was similarly assumed at 0.6 for this algorithm. The same holds for the new proposed algorithm, as well. The DBN remains the stopping criterion for the algorithm.

2.3. The Proposed Algorithm

It was established that the initial guess is drawn at the start of the optimization process by introducing a series of points, preferably, with regular arrangement across the blank contour, with the line crossing them. The initial contour is disrupted after simulation and during the correction of the blank by optimization algorithms explained in the previous section. The reason is that the points are adjusted depending on the direction of material flow, which can change the initial arrangement of the points and stop the algorithm in the following iterations. This issue is what inspired the idea behind the present algorithm. In other words, even though the material flow is not considered for correction, the contour forming after correction maintains the regularity of the points as the correction takes place only in the constrained

direction. The following discusses the new proposed algorithm, referred to as the sun-type algorithm from now on.

As evident from Fig. 4, the interval $\left|\vec{X}_{i,p}^{\,inter} - \vec{X}_{i,p}^{\,n}\right|$ is obtained by running a line through $\vec{X}_{i,p}^{\,0}$, $\vec{X}_{i,p}^{\,n}$ and finding the intersection with the target contour or point $\vec{X}_{i,p}^{\,inter}$. Then, the initial position $\vec{X}_{i,p}^{\,0}$ is corrected by, first, considering a base point $\overrightarrow{BP}$ within the die cavity, which can be more than one based on the shape and geometric complexities. In the following numerical example, the center of mass, the centroid of the die bottom surface, and even an arbitrary point on the target contour are considered as the base point. Next, the direction of correction $\vec{X}_{i,p+1}^{\,0}$ is determined by running a line over $\vec{X}_{i,p}^{\,0}$ and $\overrightarrow{BP}$, which is carried out by finding the unit vector $\widehat{UV}$ along the line and using Eq. 8.

$$UV = \frac{\overrightarrow{BP} - \vec{X}_{i,p}^{\,0}}{\left|\overrightarrow{BP} - \vec{X}_{i,p}^{\,0}\right|} \tag{8}$$

The boundary node $\vec{X}_{i,p}^{\,0}$ is then modified in the opposite direction, depending on whether $\vec{X}_{i,p}^{\,n}$ is located inside or outside of the target contour. In other words, it $\vec{X}_{i,p}^{\,n}$ falls inside the target contour, $\vec{X}_{i,p}^{\,0}$ is driven out, and vice versa. By determining the direction in which $\vec{X}_{i,p}^{\,0}$ is corrected, the displacement is obtained from Eq. 9.

$$\vec{X}_{i,p+1}^{\,0} = \vec{X}_{i,p}^{\,0} \pm \xi \left|\vec{X}_{i,p}^{\,inter} - \vec{X}_{i,p}^{\,n}\right| UV \tag{9}$$

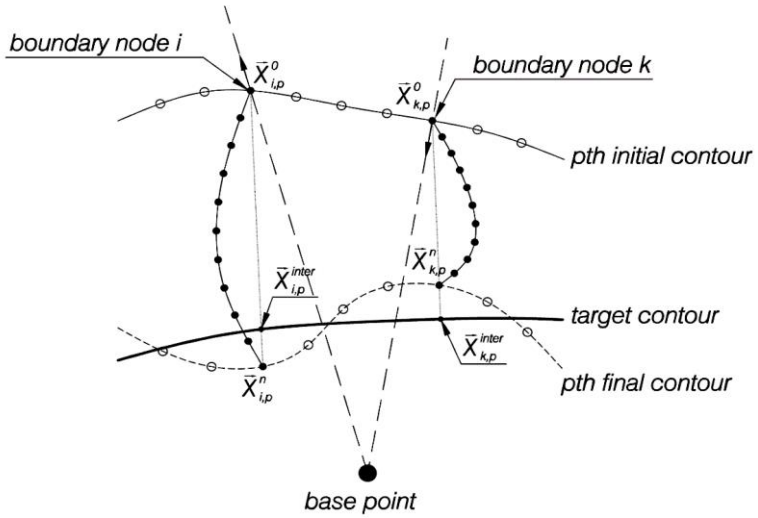

Fig. 4. The deformation path of two boundary nodes in the new proposed algorithm.

The algorithms described in in this section of the article were prepared using Python programming language as a suitable code and this code has been implemented in Abaqus software to perform numerical simulation. The written code performs the various iteration steps in the algorithms automatically. After executing the written Python code, the results of different iterations in Abaqus software can be seen and also the results of the last iteration in the simulation process show the optimal blank in the deep drawing process.

3. Performance Comparison of the Algorithms through a Numerical Example

The deep drawing process was numerically simulated in the present study by the finite element method and the commercial software, ABAQUS. Deformations were assumed to be significant, and nonlinear geometric effects were taken into account. A contact constraint was established between all surfaces in contact, and the Coulomb model of friction was applied by the penalty method. The material was assumed to have an elastic–plastic behavior regardless of strain rate and temperature effects. Before optimization begins, a suitable number of elements is found by grid analysis, investigating the effect of the grid coarseness on the changes in the sheet metal thickness. Several studies in the literature can be referred to [38] for instructions on grid analysis, which was not discussed here for conciseness.

A Python program was developed in ABAQUS to examine the efficiency of the proposed algorithm. The program ran all iterations automatically. A numerical example was considered for analysis. The results were then compared with the literature.

Several initial guesses were also considered, and the algorithm ran on different ones to investigate the effect of the initial guess. To compare the proposed algorithm with that of Fazli et al. [35] and the Push–Pull method of Hammami et al. [33], examples were drawn from the former for a better comparison.
The sheet metal was assumed to have a thickness of 0.85 mm and elastic–plastic mechanical behavior. The stress–strain behavior in the plastic region was characterized by a power-law relation of the type presented in Eq. 10. The elastic properties and the coefficients of Eq. 10 are presented in Table 1.

$$\sigma = k\,(\varepsilon_0 + \varepsilon)^n \tag{10}$$

Table 1. Mechanical properties of the blank in deep drawing. [35]

Value	Symbol	Parameter
200 Gap	$\boldsymbol{E}$	Young's modulus
0.3	$\boldsymbol{\nu}$	Poisson's ratio
514 MPa	$\boldsymbol{k}$	Stress constant
0.001	$\boldsymbol{\varepsilon_0}$	Strain constant
0.2	$\boldsymbol{n}$	Strain hardening exponent
129.11 MPa	$\boldsymbol{S_y}$	Elastic limit

Figure 5 illustrates the geometries and dimensions of the die, blank holder, and the punch. All dimensions in the figure are in millimeters (mm). The depth of drawing was 20 mm, and the target was an edge of uniform 2 mm width across the produced part. A 9800 N blank holder force was considered, which remained fixed throughout the process. The punch was assumed to travel at a 20 mm.s-1 speed. Table 2 presents the coefficients of friction between all surfaces.

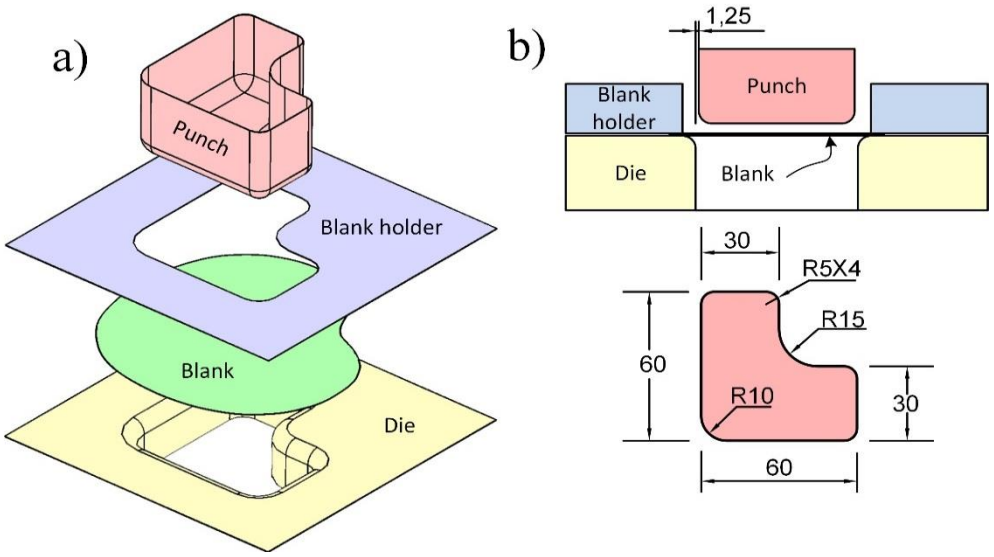

Fig. 5. The deep drawing dies geometry; a) the deep drawing die assembly, b) die dimensions.

The proposed algorithm was developed by Python programming in ABAQUS to solve the optimization problem. In this section, correction algorithms are implemented on the example separate, presenting the optimum blank contours obtained from each algorithm for comparison against the results of Fazli et al. [35]. Further, in this case, ξ was assumed at 0.6, and a mesh size of 1.5 was considered for all die components, except the blank which was modeled with a mesh size of 2.5. Moreover, the blank was not partitioned. The die, blank holder, and punch were modeled as rigid, and four-node thin shell elements were used to simulate the sheet metal deformation. Figure 6 shows the contour of the initial blank that was selected randomly and far from the shape geometry. A DBN of less than 0.5 or the number of iterations (15) was adopted as algorithm stopping criteria. These conditions hold for all algorithms. Further, the reference point for implementing the proposed in this example is the geometric center of mass. The coefficient ξ in this example is similar for all algorithms to establish similar conditions.

Table 2. Coefficients of friction between contacting surfaces in the first example. [35]

Coefficient of friction	Contacting surface
0.24	Blank and punch
0.12	Blank and die
0.12	Blank and blank holder

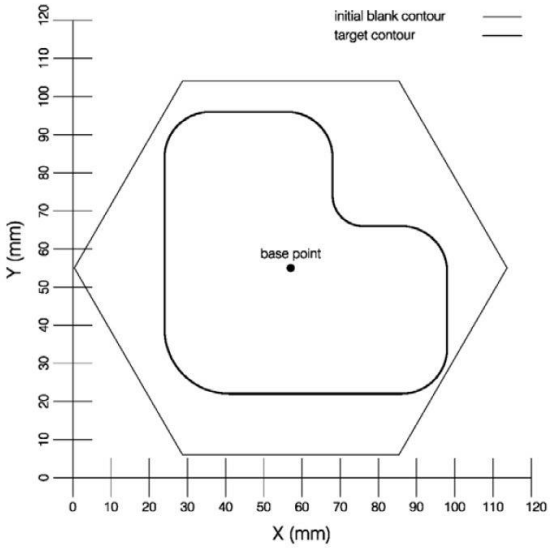

Fig. 6. The initial blank contour and the target contour selected for implementing the shape correction and optimization algorithm.

Figure 7 evaluates the final contour resulting from the forming process by Push–Pull optimization in the first three iterations, comparing the optimum blank obtained at the fifth iteration with the optimum blank from the study of Fazli et al. [35]. Given the fact that some of the following algorithms may have more iterations, only the first three iterations, as well as the final one yielding the optimum blank, are shown here.

As evident from the figure, the optimum blank is approximately similar to what was obtained by Fazli et al. [35], confirming the correctness of the simulation. Figure 7a shows the final contour obtained from the initial blank, which is much different from the target contour. Moreover, Fig. 7b shows the final contour obtained from the corrected blank after the first iteration. The final corrected blank contour resulting from the first iteration is close to the target contour with little approximation. Fig. 7c shows the final corrected contour resulting from the second iteration, which shows a negligible difference from the target contour. Finally, Fig. 7d compares the results with the optimum blank of Fazli et al. [35]. Considering that obtaining the optimum blank is contingent on the maximum distance of the boundary node on the final contour from the target contour is less than 0.5, the final and target contours align almost perfectly, which is the reason they are not illustrated in the figure.

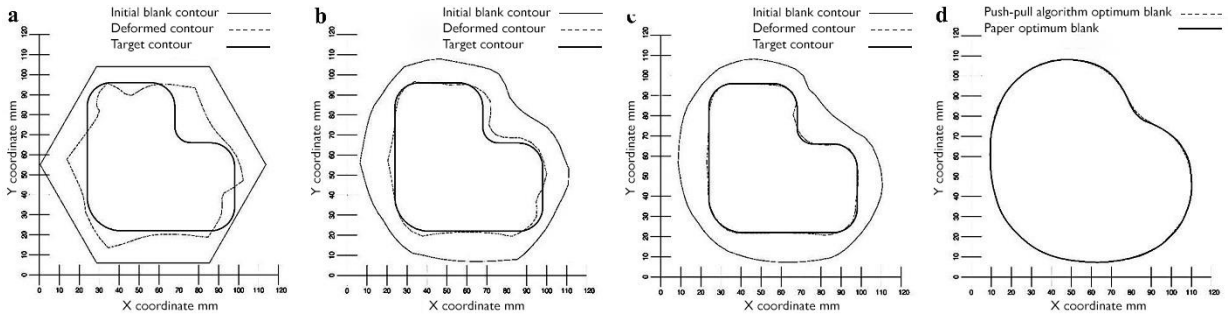

Fig. 7. Evaluation of final contour after deformation using the *Push–Pull algorithm*. (a) initial blank, (b) 1st modified blank, (c) 2nd modified blank, (d) 5th modified blank.

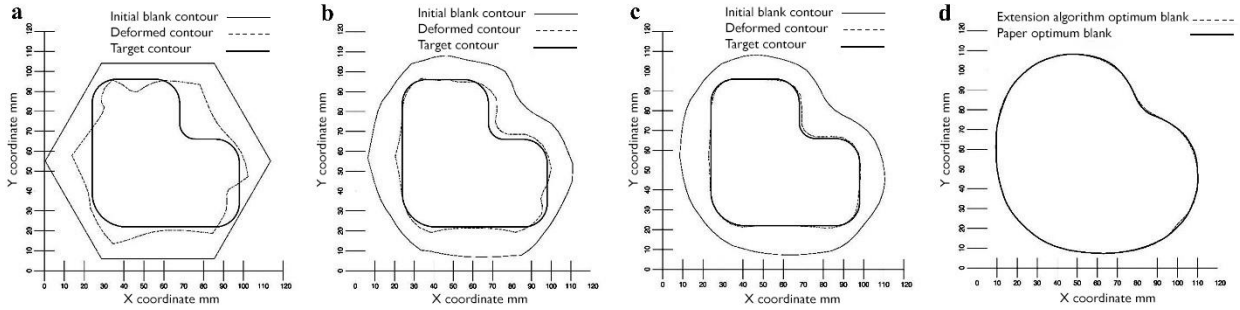

Fig. 8. Evaluation of final contour after deformation using the *Extension algorithm*. (a) initial blank, (b) 1st modified blank, (c) 2nd modified blank, (d) 5th modified blank.

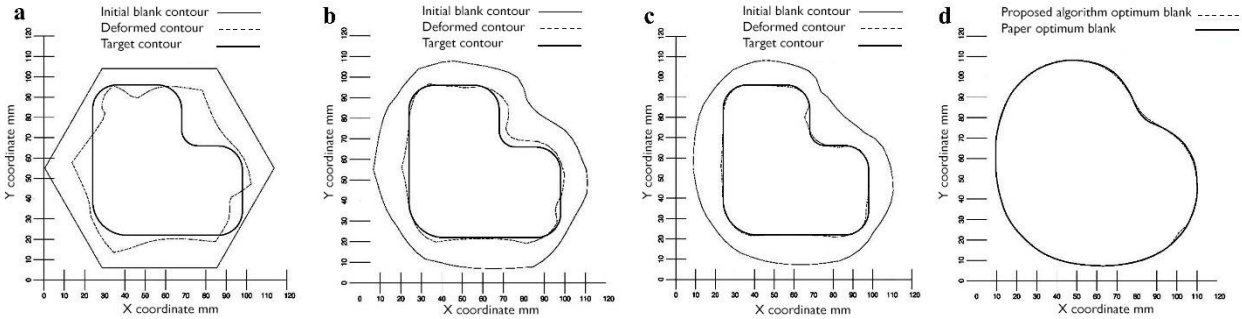

Fig. 9. Evaluation of final contour after deformation using the *proposed algorithm*. (a) initial blank, (b) 1st modified blank, (c) 2nd modified blank, (d) 4th modified blank.

Figure 8 evaluates the final contour resulting from the forming process by Extension optimization in the first three iterations, comparing the optimum blank obtained at the fifth iteration with the optimum blank from the study of Fazli et al. [35]. In this example too, the result is approximately close to the study of Fazli et al. [35]. This figure can be interpreted similarly to the previous algorithm. Therefore, the descriptions are not repeated here.

Figure 9 presents the results corresponding to the authors' proposed algorithm. This figure can be interpreted similarly to the previous algorithm. Therefore, the descriptions are not repeated here.

4. Comparing the Results of Implementing the Algorithms

In the following, the performances of the algorithms in solving the problem were compared based on the results. Table 3 shows the number of iterations that took each algorithm before reaching the stopping constraint and the optimum blank along with the maximum and mean DBN at the last iteration. The minimum wall thickness is also presented for comparison with the study of Fazli et al. [35]. As evident from the table, with fewer iterations and smaller mean and maximum error, the authors' new algorithm displayed the best performance.

Table 3. Results of implementing the algorithms.

Algorithm name	Iterations	Maximum *DBN*	Mean *DBN*	The minimum wall thickness
Push–Pull [33]	5	0.263249	0.082827	0.6570
Extension [35]	5	0.214324	0.077019	0.6558
The Proposed Algorithm	4	0.214109	0.073986	0.6464

5. Optimization of the Internal Boundary

The other new subject covered in this study is the assumption of a cavity in the initial blank and designing its initial geometry to develop into what is desired in the final product. This approach can be advantageous in the production of parts that feature cavities as the blank can be prepared with a cavity of a particular geometry that can develop the desired shape by deformation during deep drawing. This method is especially useful in cases where there is a limitation in creating holes after the drawing process. A cavity was considered inside the example to blank from Section 3 in the shape of its outer contour, and the external and internal boundaries of the blank were corrected simultaneously using the proposed algorithm. The initial guess for the external and

internal boundaries was circular. Figure 10 shows the initial guess and target contours of the external boundary, as well as the internal boundary (the cavity), for the said example. As evident, the initial guess was intentionally made much different from the shape of the target contour. The internal and external boundaries of the initial blank were modified in six iterations, starting from circular initial internal and external boundary configurations and using the authors' proposed algorithm (Fig. 11 & 12). In this problem too, ξ was assumed at 0.6, and the die components were simulated with an approximate mesh size of 1.5 mm, except for the initial blank, which was simulated with a 2.5 mm mesh and without partitioning. The stopping criteria of the program were the error of below 0.5 mm and the maximum number of fourteen iterations. Figure 13 shows the final three-dimensional form of the optimum blank after the sixth iteration.

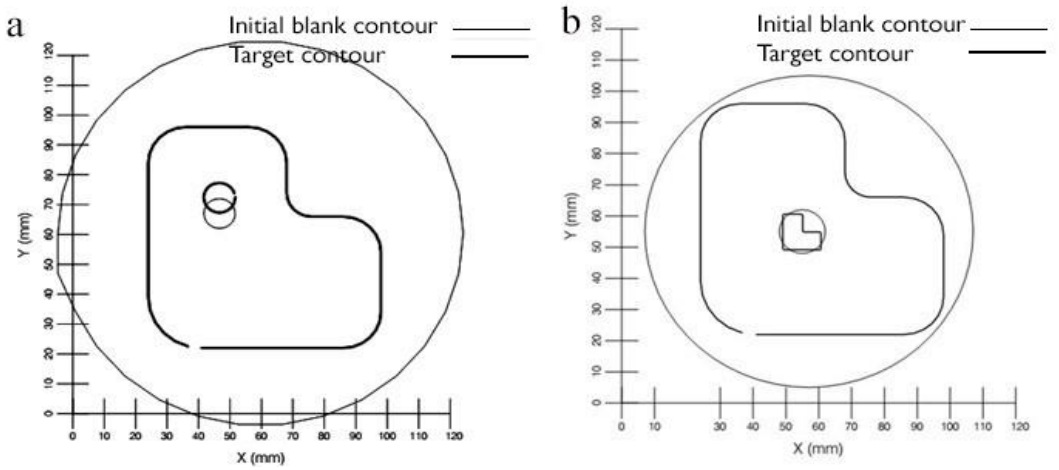

Fig. 10. The initial guess and target contours for the internal and external boundaries of the studied example. a) The target shape of the inner cavity is circular. b) The target shape of the inner cavity is L-shaped

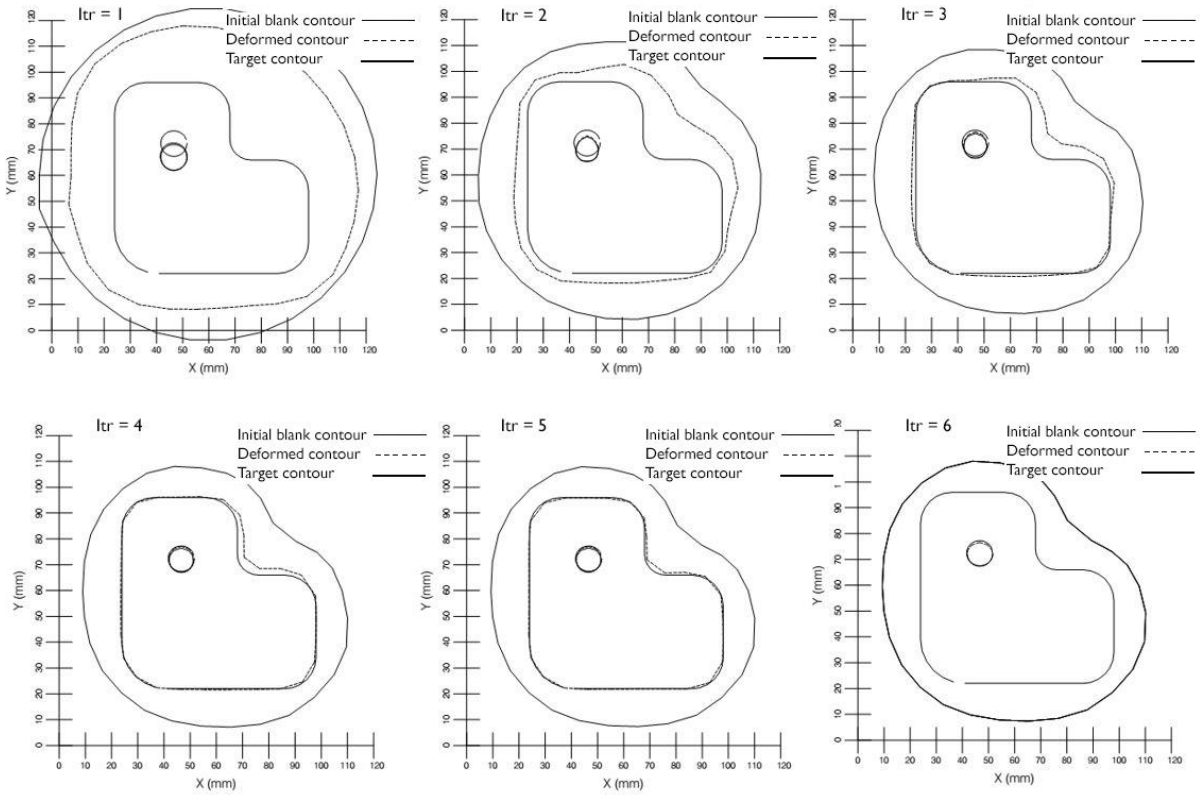

Fig. 11. The correction of the internal and external boundaries of the initial blank in six iterations, starting from the circular initial configuration and the target shape of the inner cavity is circular.

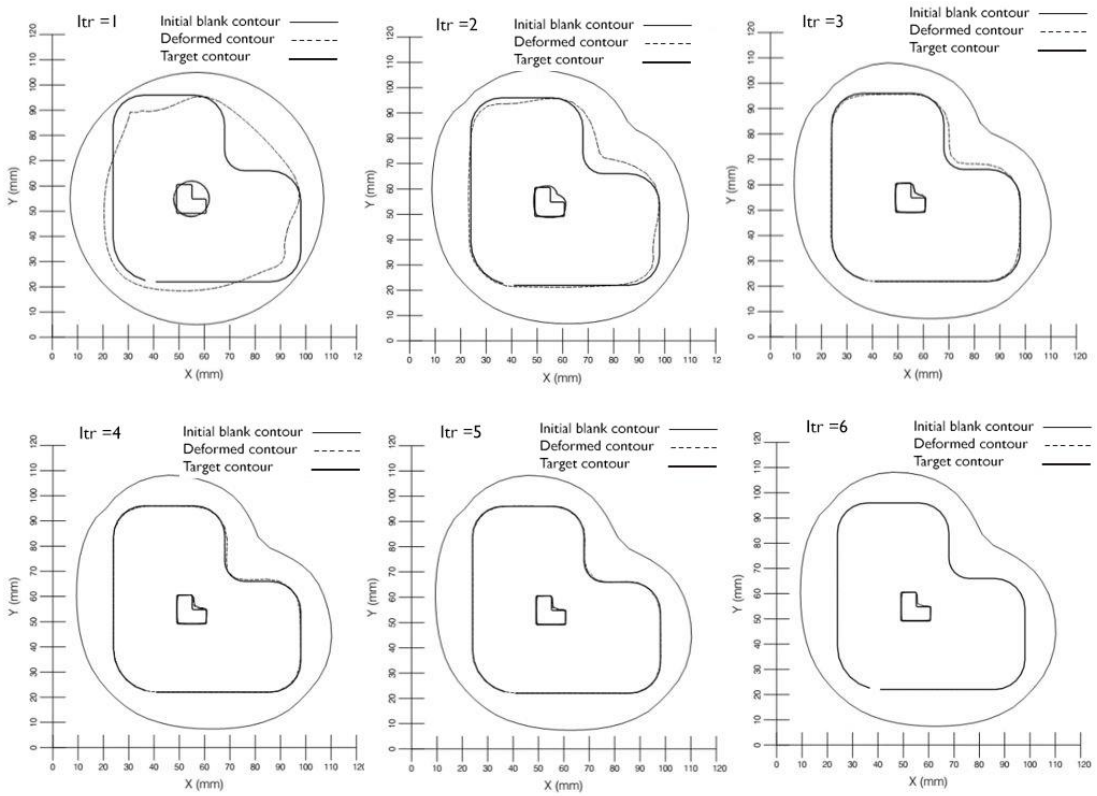

Fig. 12. The correction of the internal and external boundaries of the initial blank in six iterations, starting from the circular initial configuration and the target shape of the inner cavity is L-shaped.

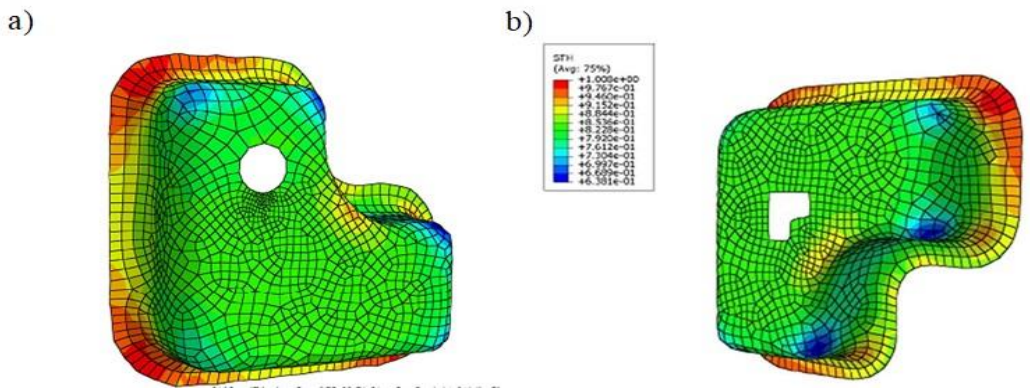

Fig. 13. The final three-dimensional shape of the optimum blank after the sixth iteration. a) The target shape of the inner cavity is circular. b) The target shape of the inner cavity is L-shaped.

6. Proof of the Efficiency of the Proposed Algorithm Against Different Initial Guesses

The problem was solved with three different initial guesses (with hexagonal, round, and square shapes) to show the efficiency of the proposed algorithm, regardless of the initial guess. Here, the initial guess was purposefully selected to be far from the optimum shape to measure the efficiency of the algorithm. In all cases, the under-relaxation factor was assumed at 0.6. The stopping criterion was considered to be when the shape error reduces under 0.5 mm at all key points.

6.1. The First Example (L-Shaped Cup Drawing)

The first example is the problem of Section 3, which was drawn from the study of Fazli et al. [35]. Figure 14 shows the correction history of the initial blank contour, in four iterations starting from the hexagonal initial shape. In this figure, the final contour resulting from each iteration is compared with the target contour. As evident, in the beginning, the final contour is away from the target due to the far-off initial guess. After the first iteration, with only one round of geometric correction, the final contour is found to have assumed the overall shape of the target

contour, getting closer to it. Further, into the process, the final contour aligns with the target contour, yielding the optimum blank configuration. It must be noted that the proposed algorithm managed to attain the optimum shape after only four iterations. The small number of iterations is an advantage to the proposed method as few iterations translate to lower computational complexity and high efficiency. After four iterations, the maximum shape error was at 0.45 mm, and the average shape error across all key points was at 0.11 mm.

Figure 15 shows a three-dimensional view of the sheet metal after the deep drawing. Figure 15a shows the final shape of the blank at the start of iterations, in which the final contour is far off the target. Figure 15b shows the final shape of the blank after four iterations.

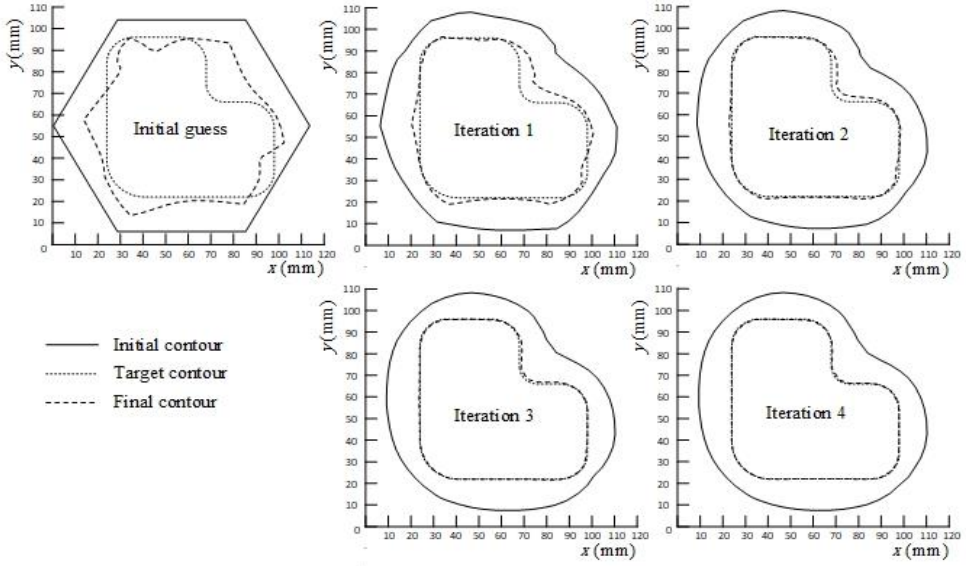

Fig. 14. Correcting the shape of the blank in four iterations, starting from the hexagonal initial shape for the first example.

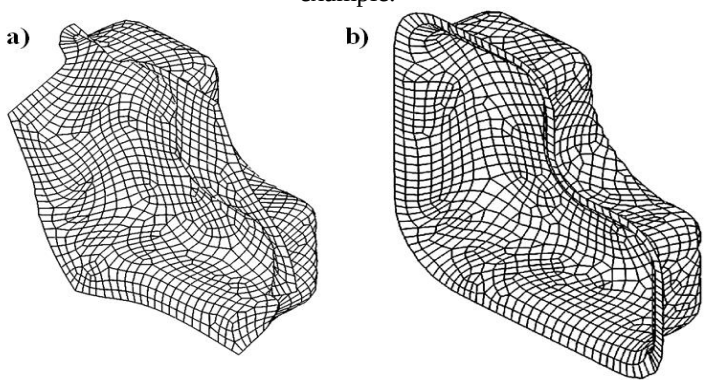

Fig. 15. A three-dimensional view of the sheet metal after the simulated deep drawing a) starting with the hexagonal initial shape, b) by the end of the fourth iteration.

The second initial guess was a circle. Figure 16a shows the changes in the initial contour after each iteration, starting from the circular initial configuration. The same figure shows the variations of the final contour throughout the iterations as well. In this case, too, the algorithm converged to the optimum in four iterations.

For the third initial guess, a square shape was considered for the blank. Figure 16b demonstrates the changes of the initial blank and the final contour, starting from the circular initial configuration. The reason for selecting the square was its substantial difference from the optimum shape. In this case, too, the final contour aligned with the target contour in four iterations.

Figure 17 plots and compares the optima obtained from three different initial guesses, as well as the optimum reported by Fazli et al. [35] for the same problem. As evident, the optimum blank obtained from the new proposed algorithm (sun-type) matches the solution offered in the said study. In other words, using different, far-off initial guesses did not affect the solution to the problem, as the result remained the same.

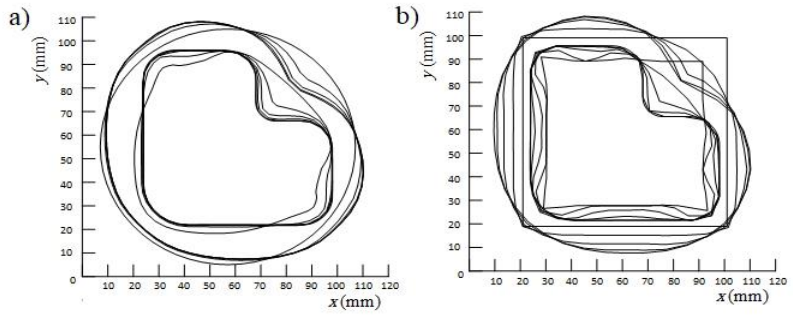

Fig. 16. The history of changes of the initial and final contours a) starting from the circular initial configuration, b) starting from the square initial configuration.

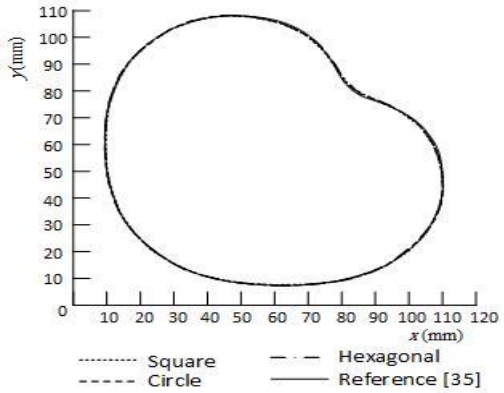

Fig. 17. The optimum blank shape was obtained based on three different initial guesses and their comparison with the results of Fazli et al. [35].

6.2. The Second Example (Oil Pan Drawing)

Another deep drawing problem with a different die and punch configuration is discussed in the second numerical example. The punch of this problem features a step at the bottom, which results in two different depths of drawing. This configuration was selected intentionally, so the efficiency of this method can be evaluated in a more complex setting. The example was drawn from the study of Fazli et al. [35], and the new algorithm was used to solve it with three different initial guesses. Figure 18 illustrates the geometrical dimensions of the die, blank holder, and punch. All dimensions in the figure are in millimeters (mm). The punch stroke was 30 mm, and the target contour was an edge of uniform 1.75 mm width across the workpiece. A 17800 N blank holder force was considered, which was assumed to remain fixed throughout the process. The punch traveled at 30 mm.s-1, and the coefficients of friction between all surfaces are presented in Table 4. Further, the under-relaxation factor was assumed at 0.6.

Similar to the previous one, in this numerical example, the problem was solved with three different initial guesses, namely circular and rectangular configurations and an irregular polygon. Figure 19a displays the three initial guesses on the same axis. Here, the initial guess was purposefully selected to be far from the optimum shape.

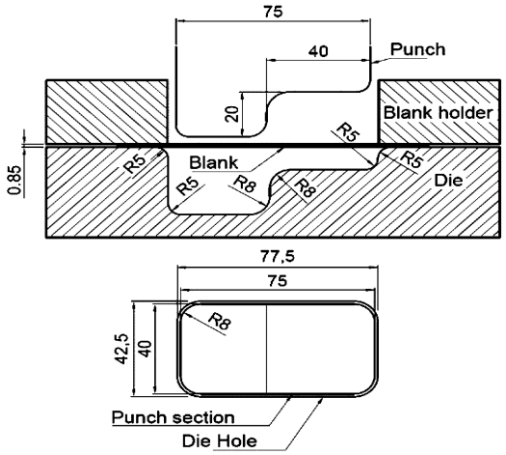

Fig. 18. Dimensions in the second example.

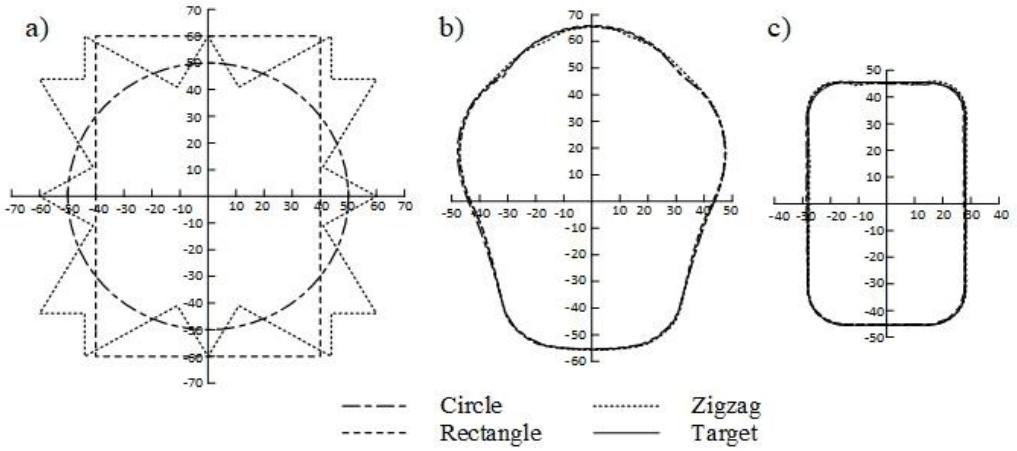

Fig. 19. The results of the second example, a) three different initial guesses, b) the optimum blank shape obtained with three different initial guesses, c) the final contour obtained from three different initial guesses.

Table 4. Coefficients of friction between contacting surfaces in the second example.

Coefficient of friction	Contacting surfaces
0.10	Blank and punch
0.05	Blank and die
0.05	Blank and blank holder

As it was mentioned earlier, in this problem, due to the more complex behavior resulting from the bottom protrusion of the punch, the number of iterations to attain the required accuracy increased to five. Figure 19b plots the initial blank contour after five iterations for each of the three initial guesses in one diagram. Figure 19c shows the final contours, as well as the target contour for all three initial guesses on the same plot. As evident, the final contour aligns with the target contour with all initial guesses. In other words, using different and far-off initial guesses had little impact on the final optimum blank configuration.

In this example, even though the initial guesses were considerably different from the optimum, the proposed algorithm managed to achieve the optimum in not more than five iterations. The small number of iterations is an advantage to the proposed method as few iterations translate to lower computational complexity and high efficiency.

Figure 20 shows a three-dimensional view of the sheet metal after the deep drawing. The same figure also shows the final blank configuration at the start of the iterations. The initial blank was circular in this case, and as evident, the final contour is much different from the target. Figure 20 shows the final blank shape after five iterations.

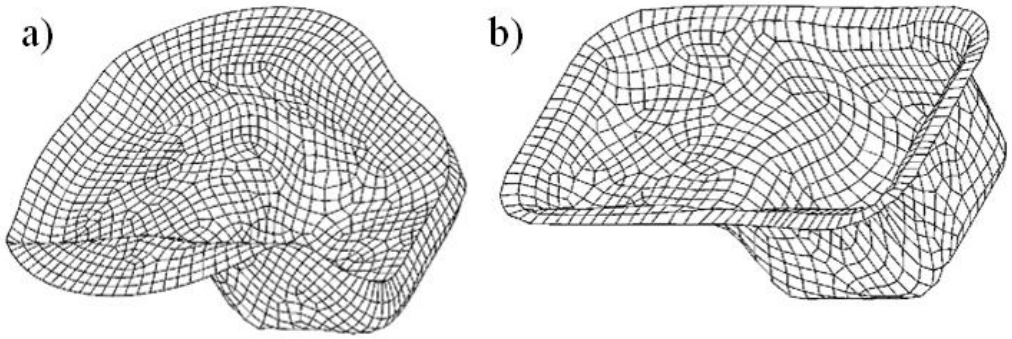

Fig. 20. A three-dimensional view of the sheet metal after the simulated deep drawing in the second example a) starting with the hexagonal initial shape, b) by the end of the fifth iteration.

7. Conclusion

The present study proposes a new blank optimization algorithm for deep drawing. The aim was to attain an algorithm that is robust against the initial guess and can find the solution to the blank optimization problem for the deep drawing process, starting from a far-off initial guess. In the proposed algorithm, the shape of the initial blank is outlined by several key points, and the iterative process starts from an initial guess and works its way up to the optimum shape. In

this algorithm, the key points are adjusted relative to a base point considered inside the die cavity, and the process continues until the stopping criterion is realized. The efficiency of the proposed method was evaluated by solving an example problem and comparing the results with two algorithms from the literature. The comparison revealed that, with the lowest average and maximum error, the proposed algorithm offers the best performance. Further, by considering a cavity inside the blank, the external and internal boundaries were corrected simultaneously as one problem using the proposed algorithm, thus proving the effectiveness of the algorithm for correcting internal boundaries as well. This approach can be advantageous in the production of parts that feature cavities as the blank can be prepared with a cavity of a particular geometry that can develop the desired shape by deformation during deep drawing. This method is especially useful in cases where there is a limitation in creating holes after the drawing process. Next, to show the robustness of the algorithm against the initial guess, two example problems were solved with three different initial guesses each, evaluating the performance of the proposed algorithm in dealing with initial guesses that are far from the optimum. The results showed that the proposed algorithm is sufficiently robust against the initial guesses for the blank, which is an advantage of the present algorithm over those from other algorithms. In the end, the present study shows that the proposed algorithm can be effectively used to solve blank optimization problems for the deep drawing process.

References

[1] V.V. Hazek, K. Lange, "Use of the slip-line method in deep drawing of large irregular shaped components", in: Proceedings of the 7th North American Metalwork Research Conference, SME, 1979, pp. 65–71.

[2] K. Lange, H. Gloeckl, "Computer aided design of blanks for deep drawn irregular shaped components", in: Proceedings of the 11th North American Manufacturing Research Conference, SME, 1983, pp. 243–251.

[3] R. Sowerby, N. Chandrasekharan, X. Chen, M. Rooks, P. Correa, "the development of computer aids for sheet metal stampings", in: S.K. Ghosh, A. Niku-Lari (Eds.), CAD/CAM and FEM in Metal working, 3rd International Conference on SAS, Pergamon Press, 1988, p.187.

[4] M. Karima, "Blank development and tooling design for drawn parts using a modified slip line field based approach", J. Eng. Ind. Trans. ASME 111, 1989, pp 345–350. https://doi.org/10.1115/1.3188770.

[5] J.H. Vogel, D. Lee, "An analytical method for deep drawing process design", Int. J. Mech. Sci. 32 (11), 1990, pp 891-907. https://doi.org/10.1016/0020-7403(90)90062-N.

[6] X. Chen, R. Sowerby, "The development of ideal blank shapes by the method of plane stress characteristics", Int. J. Mech. Sci. 2, 1992, pp.159-166. https://doi.org/10.1016/0020-7403(92)90080-Z.

[7] X. Chen, R. Sowerby, "Blank development and the prediction of earing in cup drawing", Int. J. Mech. Sci. 38, 1996, pp. 509–516. https://doi.org/10.1016/0020-7403(95)00068-2.

[8] T. Kuwabara, W.H. Si, "PC-based blank design system for deep drawing irregularly shaped prismatic shells with arbitrarily shape flange", J. Mater. Process Technol. 63, 1997, pp. 89–94. https://doi.org/10.1016/S0924-0136(96)02605-2.

[9] M.H. Parsa, P.H. Matin, M.M. Mashhadi, "Improvement of initial blank shape for intricate products using slip line field", J. Mater. Process. Technol. 145, 2004, pp. 21–26. https://doi.org/10.1016/S0924-0136(03)00858-6.

[10] N. Kim, S. Kobayashi, "Blank design in rectangular cup drawing by an approximate method", Int. J. Mach. Tool. Des. Res. 26, 1986, pp. 125–135. https://doi.org/10.1016/0020-7357(86)90213-1.

[11] Sowerby, R., Duncan, J. L. and Chu, E., "The modeling of sheet metal stampings", Int. J. Mech. Sci., 28, 1986, pp. 415-430. https://doi.org/10.1016/0020-7403(86)90062-7.

[12] Blount, G. N. and Fischer, B. V., "Computerized blank shape prediction for sheet metal components having doubly-curved surfaces", Int. J. Prod. Res., 33, 1995, pp. 993-1005. https://doi.org/10.1080/00207549508930190.

[13] A.M. Zaky, A.B. Nassr, M.G. El-Sebaie, "Optimum blank shape of cylindrical cups in deep drawing of anisotropic sheet metal", J. Mater. Proc. Technol. 76, 1998, pp. 203–211. https://doi.org/10.1016/S0924-0136(97)00349-X.

[14] K. Chung, O. Richmond, "Ideal forming II. Sheet forming with optimum deformation", Int. J. Mech. Sci. 34, 1992, pp. 617–633. https://doi.org/10.1016/0020-7403(92)90059-P.

[15] Iseki, H. and Sowerby, R., "Determination of the optimal blank shape when deep drawing non axisymmetric cups using a finite element method", Jap. Soc. Mech. Engrs Int., A, 38, 1995, pp. 473-479. https://doi.org/10.1299/jsmea1993.38.4_473.

[16] Barlat, O., Batoz, J. L., Guo, Y. Q., Mercier, F., Naceur, H. and Knopf-Lenoir, C., "Optimum blank design of blank contours using the inverse approach

and a mathematical programming technique", In Proceedings of Numisheet, 96, 1996, pp. 178-185.
[17] Lee, C. H. and Huh, H., "Blank design and strain prediction of automobile stamping parts by an inverse finite element approach", J. Mater. Proc. Technol., 63, 1997, pp. 645-650. https://doi.org/10.1016/S0924-0136(96)02700-8.
[18] Y.Q. Guo, J.L. Batoz, H. Naceur, S. Bouabdallah, F. Mercier, O. Barlet, "Recent developments on the analysis and optimum design of sheet metal forming parts using a simplified inverse approach", Comput. Struct. 78, 2000, pp. 133–148. https://doi.org/10.1016/S0045-7949(00)00095-X.
[19] T.W. Ku, H.J. Lim, H.H. Choi, S.M. Hwang, B.S. King, "Implementation of backward tracing scheme of the FEM to blank design in sheet metal forming", J. Mater. Proc. Technol. 111, 2001, pp. 90–97. https://doi.org/10.1016/S0924-0136(01)00518-0.
[20] H. Naceur, Y.Q. Guo, J.L. Batoz, "Blank optimization in sheet metal forming using an evolutionary algorithm", J. Mater. Proc. Technol. 151, 2004, pp. 183–191. https://doi.org/10.1016/j.jmatprotec.2004.04.036.
[21] Z.Y. Cai, M.Z. Li, H.M. Zhang, "A simplified algorithm for planar development of 3D surface and its application in the blank design of sheet metal forming", Finite Elem. Anal. Des. 43, 2007, pp. 301–310. https://doi.org/10.1016/j.finel.2006.10.005.
[22] M.H. Parsa, P. Pournia, "Optimization of initial blank shape predicted based on inverse finite element method", Finite Elem. Anal. Des. 43, 2007, pp. 218–233. https://doi.org/10.1016/j.finel.2006.09.005.
[23] R. Azizi, A. Assempour, "Applications of linear inverse finite element method in prediction of the optimum blank in sheet metal forming", Mater. Des. 29, 2008, pp. 1965–1972. https://doi.org/10.1016/j.matdes.2008.04.015.
[24] R. Azizi, "Different implementations of inverse finite element method in sheet metal forming, Mater", Des. 30, 2009, pp. 2975–2980. https://doi.org/10.1016/j.matdes.2008.12.022.
[25] C.H. Toh, S. Kobayashi, "Deformation analysis and blank design in square cup drawing", Int. J. Mach. Tool Des. Res. 25, 1985, pp. 15–32. https://doi.org/10.1016/0020-7357(85)90054-X.
[26] K. Chung, F. Barlat, J.C. Brem, D.J. Lege, O. Richmond, "Blank shape design for a planar anisotropic sheet based on ideal forming design theory and FEM analysis", Int. J. Mech. Sci. 39, 1997, pp. 105–120. https://doi.org/10.1016/0020-7403(96)00007-0.
[27] S.H. Park, J.W. Yoon, D.Y. Yang, Y.H. Kim, "Optimum blank design in sheet metal forming by the deformation path iteration method", Int. J. Mech. Sci. 41, 1999, pp. 1217–1232. https://doi.org/10.1016/S0020-7403(98)00084-8.
[28] V. Pegada, Y. Chun, S. Santhanam, "an algorithm for determining the optimal blank shape for the deep drawing of aluminum cups", J. Mater. Proc. Technol. 125–126, 2002, pp. 743–750. https://doi.org/10.1016/S0924-0136(02)00382-5.
[29] H. Shim, K. Son, "Optimal blank shape design by the iterative sensitivity method", Proc. IMECHE Part B J. Eng. Manuf., 216, 2002, pp. 867–878. https://doi.org/10.1243/095440502320192996.
[30] K.C. Son, H.B. Shim, "Optimal blank shape design using the initial velocity of boundary nodes", J. Mater. Process. Technol. 134, 2003, pp. 92–98.
[31] A. Vafaeesefat, "Optimum blank shape design in sheet metal forming by boundary projection method", Int. J. Mater. Form. 1, 2008, pp. 189–192. https://doi.org/10.1007/s12289-008-0023-2.
[32] M. Azaouzi, H. Naceur, A. Delame´ziere, J.L. Batoz, S. Belouettar, "a heuristic optimization algorithm for the blank shape design of high precision metallic parts obtained by a particular stamping process", Finite Elem. Anal. Des. 44, 2008, pp. 842–850. https://doi.org/10.1016/j.finel.2008.06.008.
[33] W. Hammami, R. Padmanabhan, M.C. Oliveira, H. BelHadjSalah, J.L. Alves, L.F. Menezes, "A deformation based blank design method for formed parts", Int. J. Mech. Mater. Des. 5, 2009, pp. 303–314. https://doi.org/10.1007/s10999-009-9103-9.
[34] R. Padmanabhan, M.C. Oliveira, A.J. Baptista, J.L. Alves, L.F. Menezes, "Numerical study on the influence of initial anisotropy on optimal blank shape", Finite Elem. Anal. Des. 45, 2009, pp. 71-80. https://doi.org/10.1016/j.finel.2008.07.012.
[35] A. Fazli, B. Arezoo, "A comparison of numerical iteration based algorithms in blank optimization", Finite Elem. Anal. Des., 50, 2012, pp. 207-216. https://doi.org/10.1016/j.finel.2011.09.011.
[36] M.J. Kazemzadeh-Parsi, "Numerical flow simulation in gated hydraulic structures using smoothed fixed grid finite element method", Applied Mathematics and Computation, Vol. 246, 2014, pp. 447-459.
[37] M.J. Kazemzadeh-Parsi and F. Daneshmand, "Inverse geometry heat conduction analysis of functionally graded materials using smoothed fixed grid finite element method", Inverse problems in Science and Engineering, Vol. 21, No. 2, 2013, pp. 235-250.
[38] Liu T. Itoh, "Numerical Techniques for Microwave and Millimeter and Millimeter-Wave Passive Structures", Second Edition, New York: Wiley, 1989, pp. 305-320,

[39]. W. Zhanga, J. Gaob, J. Caob, "Blank geometry design for carbon fiber reinforced plastic (CFRP) preforming using finite element analysis (FEA)", Procedia Manufacturing 48, 2020, pp. 197–203. https://doi.org/10.1016/j.promfg.2020.05.038

[40]. S. Yaghoubi, F. Fereshteh-Saniee, "Optimization of the geometrical parameters for elevated temperature hydro-mechanical deep drawing process of 2024 aluminum alloy", Proc IMechE Part E: J Process Mechanical Engineering, 0(0), 2020, pp. 1–11. https://doi.org/10.1177/0954408920949364

[41]. M. Ghasemabadian, M. Kadkhodayan, W. Altenhof, "Experimental, numerical, and multi-objective optimization investigations on the energy absorption features of single- and bi-layer deep-drawn cups", Proc IMechE Part L: J Materials: Design and Applications, 0(0), 2020, pp. 1–22. https://doi.org/10.1177/1464420720972431